Progress In Electromagnetics Research M, Vol. 101, 25–35, 2021

Spoof Surface Plasmon Polaritons and Half-Mode Substrate Integrated Waveguide Based Compact Band-Pass Filter for RADAR Application

Keyur Mahant[1], Hiren Mewada[2], Amit Patel[1, *], Alpesh Vala[1], and Jitendra Chaudhari[1]

Abstract—A band-pass filter using spoof surface plasmon polaritons (SSPPs) and half-mode substrate integrated waveguide (HMSIW) for Ka-band RADAR application is proposed. In order to achieve the band-pass response, an HMSIW structure with high pass response and SSPPs with band-stop response are combined. Moreover, to investigate effects of geometric dimensions on the frequency characteristics of the proposed band-pass filter are examined by parametric analysis. It has been observed that lower cut-off and upper frequencies can be individually controlled just by changing the structural parameters. High Frequency Structure Simulator (HFSS) software was utilized to simulate the proposed structure. HFSS is the simulation tool for complex 3-D geometries and uses the finite element method (FEM). To validate the functionality, the proposed band-pass filter is fabricated on the dielectric material RT duroid 5880 with the dielectric constant $\varepsilon_r = 2.2$, height $h = 0.508$ mm, and dissipation factor $\tan\delta = 4 \times 10^{-4}$. The measured result shows return loss better than -10 dB and insertion loss less than 1.25 dB with the 3 dB fractional bandwidth (FBW) of 44.02% at the center frequency of 7.95 GHz.

1. INTRODUCTION

Radio detection and ranging (RADAR) measures the distance, speed, and the position of an object using electromagnetic waves. In paper [1], traffic RADAR was proposed to measure the speed of the vehicle by measuring the phase shift of the transmitted and reflected signals. Nowadays, various bands from X band to Ka-band are utilized to measure the speed of the vehicles [2]. In the proposed system, Ka-band Step Frequency Continuous Wave (SFCW) RADAR operating from 26 to 36 GHz frequency band is presented. The configuration of the proposed system is shown in Figure 1. In the proposed system, frequency synthesizer is utilized for the generation of signal operating from 6.5 to 9 GHz frequency band. In order to remove generated harmonics, a band-pass filter is designed. The designed HMSIW and SSPPs based filter is emphasized by red dotted lines in Figure 1, operating from 6.5 to 9 GHz frequencies.

Conventionally, microstrip lines and waveguides are utilized for the design and development of the microwave and millimetre wave circuits. Waveguides are bulky, costly, and difficult to fabricate, whereas microstrip lines have low quality factor, low power handling capacity, and are quite lossy [3, 4]. SIW structures offer the advantage of typical metallic rectangular waveguides like low insertion loss, huge power handling ability, and high quality factor. Moreover, SIW also exhibits the advantages of microstrip lines such as low fabrication cost, light weight, and ease of integration [5, 6]. However, there is a further scope to decrease the size of the SIW structure. In order to reduce the size of these structures, concept of half-mode SIW (HMSIW) was introduced. The HMSIW technique decreases the size of the

Received 18 December 2020, Accepted 2 February 2021, Scheduled 9 February 2021

* Corresponding author: Amit Patel (amitvpatel@charusat.ac.in).

[1] CHARUSAT Space Research and Technology Center, V. T. Patel Department of Electronics and Communication Engineering, Charotar University of Science and Technology Changa, India. [2] Prince Mohammad Bin Fahd University, Al Khobar, Kingdom of Saudi Arabia.

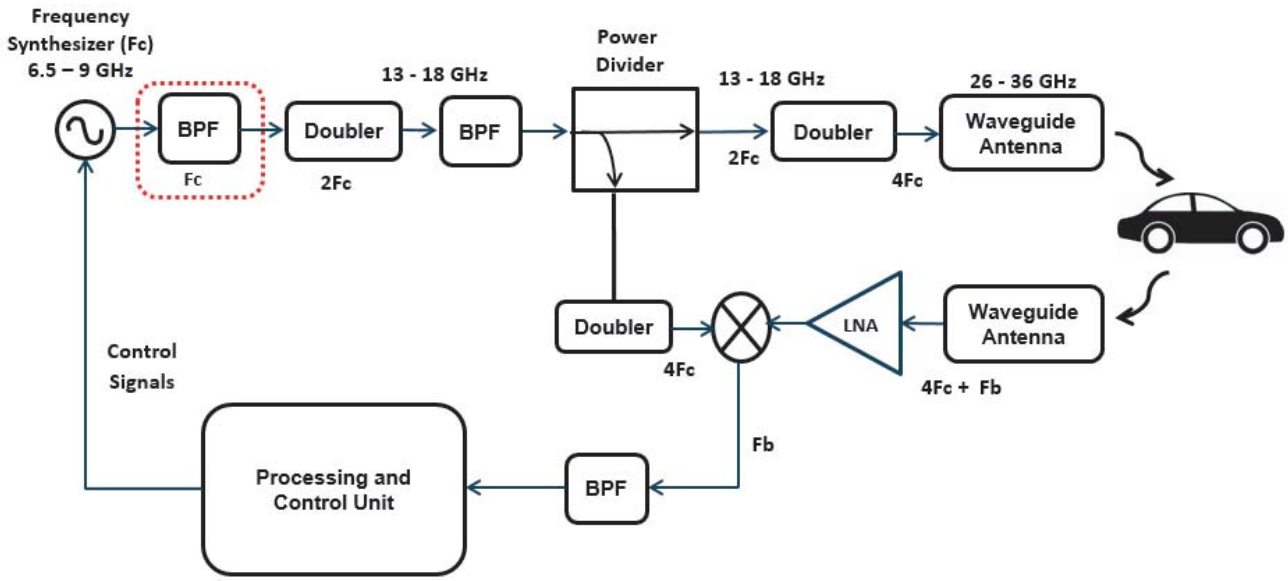

Figure 1. Ka-band RADAR system configuration.

structure by half while maintains the characteristics of the SIW technique. In a typical SIW structure, an e-field is concentrated at the center of the vertical plane in the direction of wave propagation. Thus, vertical plane of the SIW structure can be deliberated as a magnetic wall, and HMSIW structure is achieved by bifurcating the SIW structure from the vertical plane.

Plasmons are oscillation of electron, excited by the electromagnetic radiation origins conversion of photons into plasmons. Surface plasmons are the plasmons propagating at the metal-dielectric interface. Usually, plasmonic metamaterial has a metal surface with the array of subwavelength grooves. Surface plasmon polaritons (SPPs) are the surface electromagnetic wave propagating on the surface of the interface between metal and medium at visible and ultraviolet (UV) frequencies [7, 8]. However, SPPs are not excited at the lower frequencies (microwave, millimetre wave, and terahertz) as metals act as a perfect electrical conductor (PEC) at lower frequencies. Spoof surface plasmon polaritons (SSPPs) are the electromagnetic surface wave, which supports a similar behaviour to SPPs at microwave frequency [9, 10]. Moreover, dispersion characteristics and cut-off frequency can be controlled just by changing the geometry of the structure. Thus, SSPPs attract many investigators in the field of microwave and millimetre wave.

HMSIW structure exhibits a high-pass response, while SSPPs have band-stop response. These two structures are combined to realize the ultra-wideband band-pass response. Here, SSPP structure is realized by etching arrays of sub-wavelength grooves on the upper metallic plate. To validate the simulation results, the proposed design was fabricated and tested.

2. DESIGN AND ANALYSIS

As stated previously, designing an ultra-wideband band-pass filter is realised by etching SSPPs on the top metallic plane of an HMSIW structure. The proposed filter is designed and fabricated using RT duroid 5880 dielectric material having dielectric constant (2.2) and height (0.508 mm). Moreover, simulations and optimization of the proposed structure have been conducted using commercial software Ansoft HFSS.

2.1. Design of Basic HMSIW Structure

As mentioned above, the SIW structure is formed by top and bottom metallic plates with a central less lossy dielectric layer inserted with two linear sequences of metallic via joining upper and lower metallic

plates. The SIW structure has electromagnetic features equivalent to the conventional waveguide. Furthermore, various parameters of the HMSIW structure such as width, length, and cut-off frequency can be calculated with Equations (1), (2), and (3) correspondingly, which is mentioned in [5, 6].

$$f_{cTE_{0.5,0}} = \frac{Co}{2\sqrt{\varepsilon_r}}\left(a - \frac{4R^2}{0.95P}\right)^{-1} \tag{1}$$

$$W_{eff} = W_{SIW} - \frac{D^2}{0.95P} \tag{2}$$

$$L_{eff} = L_{SIW} - \frac{D^2}{0.95P} \tag{3}$$

where C_0 is the speed of light in free space; a is the width of the SIW; R is the via radius; and P is the via spacing.

Figure 2(a) shows the proposed HMSIW filter. The detailed dimensions of the structure are tabulated in Table 1. The S-parameter simulation result is shown in Figure 2(b), which shows that the HMSIW structure has high pass response with the cut-off frequency of 5.8 GHz, insertion loss better

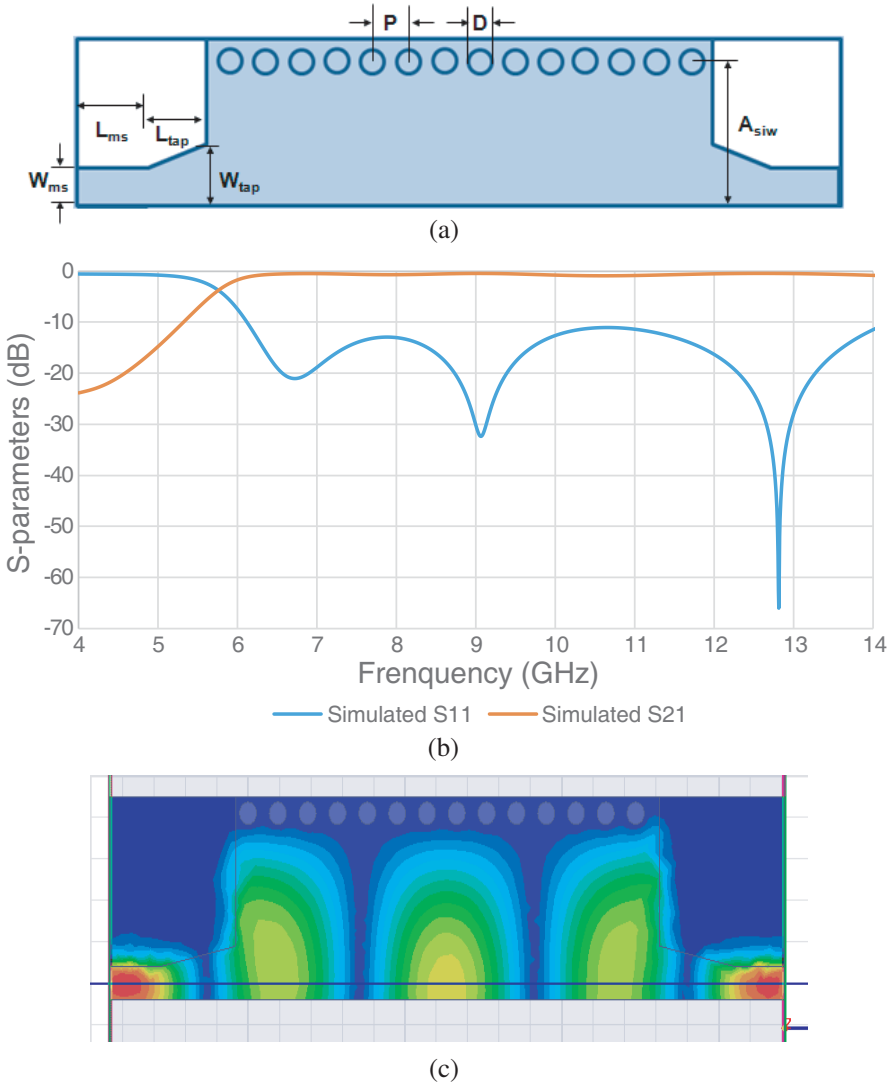

Figure 2. The proposed HMSIW structure. (a) Schematic view (blue colour region represents copper). (b) S-parameter simulation results and (c) E-field distribution.

Table 1. Dimensions of the proposed filter shown in Figure 2(a).

Parameter	Values in mm
Via Diameter (D)	1.10
Via Pitch (P)	2.00
Width of SIW (A_{SIW})	8.22
Microstrip Width (W_{ms})	1.56
Microstrip Length (L_{ms})	3.10
Taper Width (W_{tap})	3.60
Taper Length (L_{tap})	4.90

than 0.5 dB, and return loss more than 12 dB within the preferred operating frequency band. Moreover, the E-field distribution in the proposed structure is shown in Figure 2(c). It is very clear that the E-field distribution in HMSIW is same as half of the fundamental $TE_{1,0}$ mode in the typical SIW structure.

2.2. Design of HMSIW and SSPPs Based Wide Band Band-Pass Filter

To begin with, it has been observed that HMSIW structure exhibits the high-pass response, presented in Figure 2(b). Band-pass response in the SIW structure can be achieved by utilizing several techniques such as inductive post based filter, defected ground structure, split-ring resonators, and stepped impedances [11–17]. However, a wide-band band-pass filter with SSPPs outstrips the other approaches because of ease of frequency tuning and implementation in HMSIW structure. By combining the HMSIW structure with high-pass response and SSPPs with stopband response, a compact ultra-wideband band-pass filter is realized. In the presented band-pass filter, the SSPP structure is achieved by etching arrays of sub-wavelength grooves on the top metallic layer. Proposed design of the wide-band band-pass filter is shown in Figure 3(a). As shown in Figure 3(d), HMSIW structure has fast-wave fundamental mode while SSPPs structure has slow-wave mode. The lower cut-off frequency for the HMSIW structure is $f1 = 5.8$ GHz, and the upper cut-off frequency of the SSPPs is $f2 = 12.7$ GHz. In the proposed structure, sub-wavelength corrugated grooves were etched on the top metallic plane of the HMSIW structure to achieve the slow-wave behaviour. The width of the SIW structure is set to

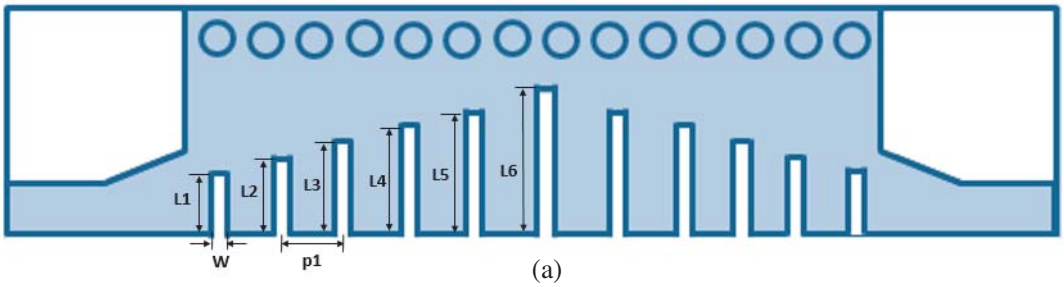

(a)

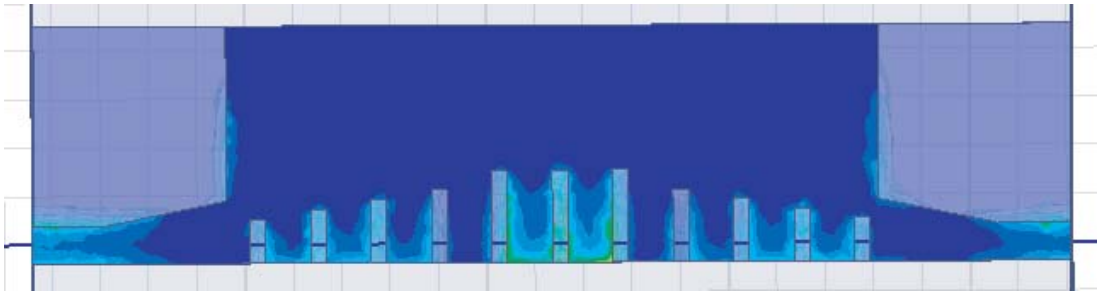

(b)

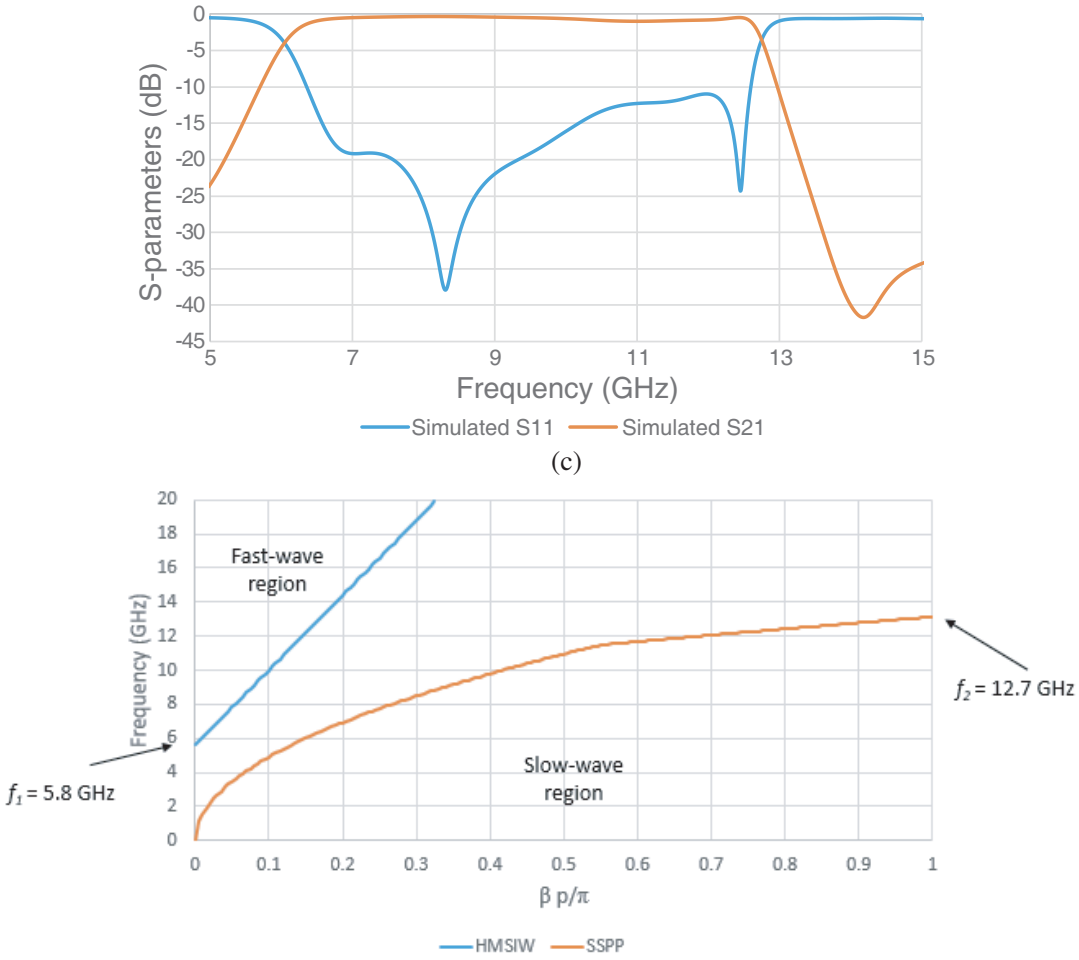

Figure 3. (a) Proposed wide band band-pass filter. (b) E-field distribution. (c) S-parameter simulation results and (d) dispersion diagram.

8.22 mm while the length of the vertical slot (L) is set to 4.2 mm based on the dispersion diagram in Figure 3(d). The length, width, and pitch of the corrugated grooves are L, w, and $p1$, respectively. The width (w) and pitch ($p1$) of the corrugated grooves are selected such that they support slow-wave mode at microwave frequencies, and it is much less than guided wavelength and in the order of sub-wavelength of the operating frequency. The detailed dimensions of the structure are tabulated in Table 2. The simulation result shows a return loss better than −10 dB and insertion loss less than 1.25 dB with the 3 dB fractional bandwidth (FBW) of 71.65% (6 GHz to 12.7 GHz) at the center frequency of 9.35 GHz as shown in Figure 3(c). Moreover, electric field distribution in the designed filter is shown in Figure 3(b). The dispersion characteristics of the SSPP is defined by the equation mentioned below:

$$\beta = \kappa_0 \sqrt{1 + \frac{w^2}{p1^2} \tan^2(\kappa_0 L)} \tag{4}$$

where $\kappa_0 = \omega/c$, κ_0 = wave vector in vacuum, ω = angular frequency, and β is the propagation constant.

To investigate, the influences of physical dimension on frequency characteristics various parameters like width of SIW (A_{SIW}), length of the corrugated grooves (L), and width of the corrugated grooves (w) are varied. It has been observed that lower and upper cut-off frequencies can be done individually by varying the filter dimensions.

2.3. Effect of Physical Dimension on Frequency Characteristics with Traditional SSPPs

It has been observed that lower cut-off frequencies can be independently controlled by changing the width of SIW (A_{SIW}) while upper cut-off frequencies are controlled just by changing either the length

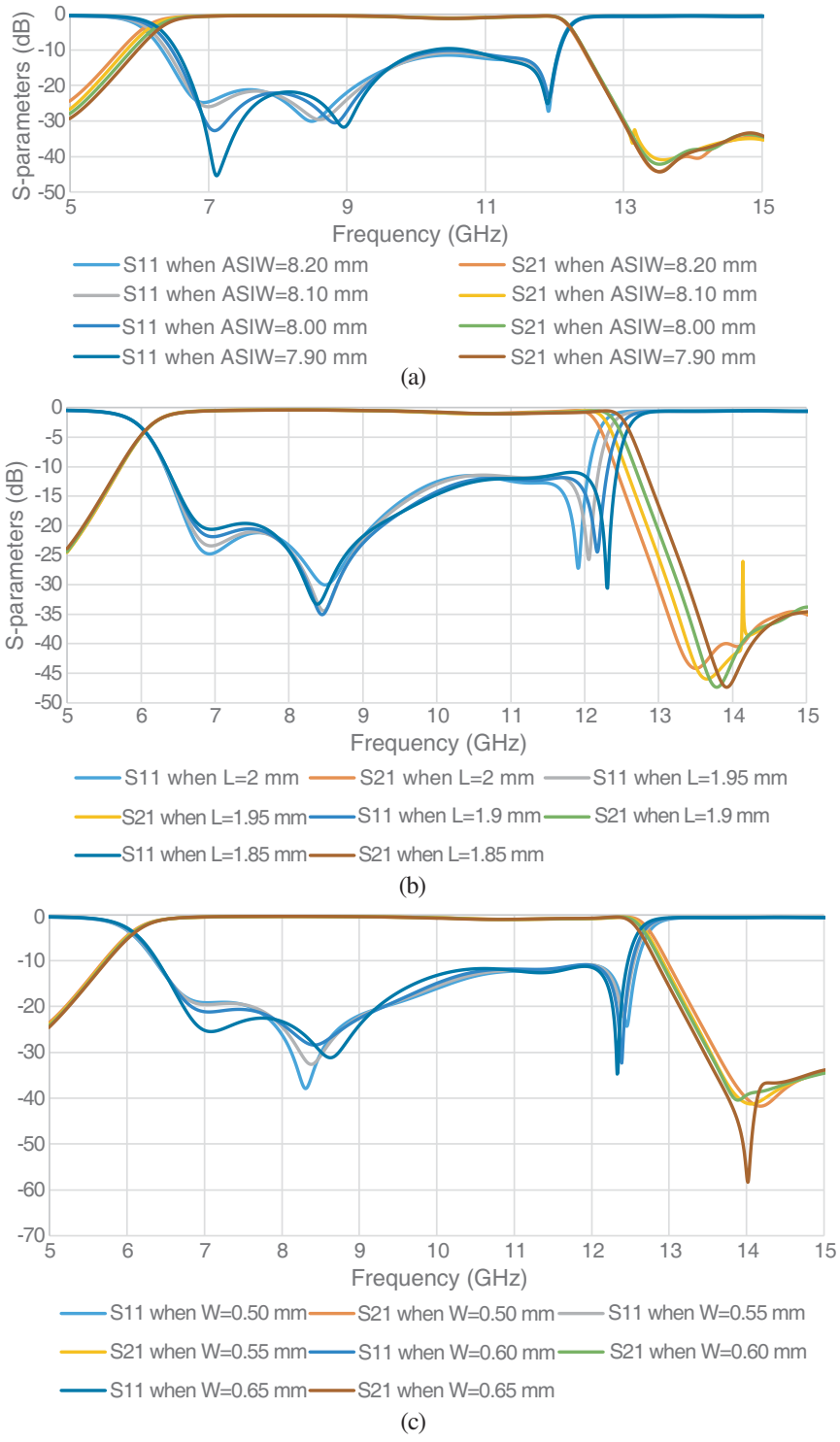

Figure 4. Simulation results. (a) Effect of width of SIW (A_{SIW}). (b) Length of the corrugated grooves (L) and (c) width of the corrugated grooves (W).

Table 2. Designed SSPPs parameters (Unit: Millimeter).

L1	**L2**	**L3**	**L4**
1.8	2.2	2.6	3
L5	**L6**	**w1**	**w2**
3.8	4.2	1.6	1

of the corrugated grooves (L) or the width of the corrugated grooves (W). The simulated S-parameter results obtained by changing the various above mentioned parameters are shown in Figure 4.

2.4. Effect of Modified Hockey Stick-Shaped SSPPs Structure on Frequency Characteristics

Initially, simulation results show the return loss better than −10 dB and insertion loss less than 1.25 dB with the 3 dB fractional bandwidth (FBW) of 71.65% at the center frequency of 9.35 GHz. In order to achieve the narrow-band response, to meet system specification an SSPPs structure is modified. The modified hockey stick-shaped SSPPs (HSS-SSPPs) structure are introduced into the HMSIW structure as shown in Figure 5(a). Firstly, a $w1$ slot was inserted in the structure. It was observed that as the $w1$ slot is inserted in the SSPPs structure, the inductance of the circuit increases, and the cut-off frequency decreases, as shown in Figure 5(c). Furthermore, inductance can be increased by increasing the area of $w1$ slot. Moreover, overall capacitance of the structure is increased by inserting the $w2$ slot, which leads to decrease of the cut-off frequency. Consequently, the desired band of operation (6.5 to 9 GHz) is achieved.The simulation result shows the the return loss better than −10 dB and insertion loss less than 1 dB with the 3 dB fractional bandwidth (FBW) of 44.58% at the center frequency of 7.85 GHz, and the effects of $w1$ and $w2$ slots are shown in Figure 5(c). Moreover, electric field distribution in the designed filter is shown in Figure 5(b). Furthermore, frequency tuning is also possible in the proposed modified HSS-SSPPs structure by varying the physical dimension of the proposed structure like length of the corrugated grooves (L) and width of the corrugated grooves (W). The simulation results of effect of width of the corrugated grooves (W) on S-parameter are presented in Figure 5(d). It has been observed that upper cut-off frequencies can be easily controlled just by either changing the width of the corrugated grooves (W) or changing the length of the corrugated grooves (L).

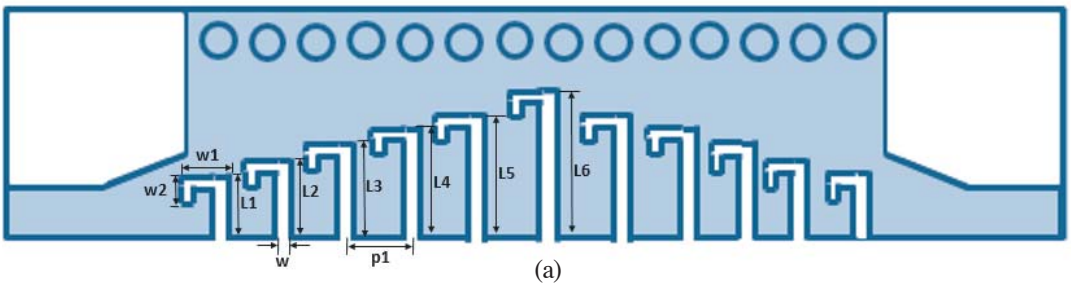

(a)

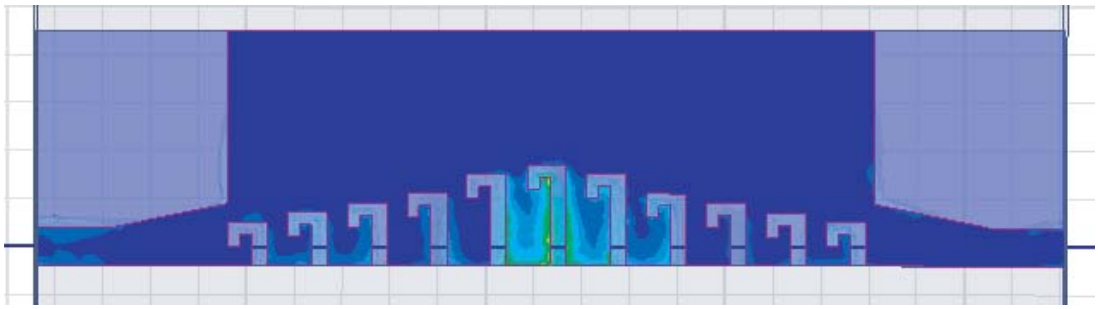

(b)

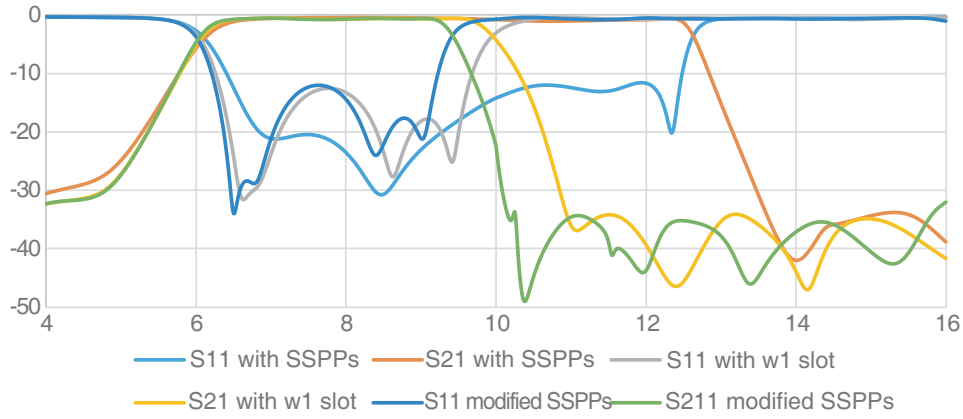

(c)

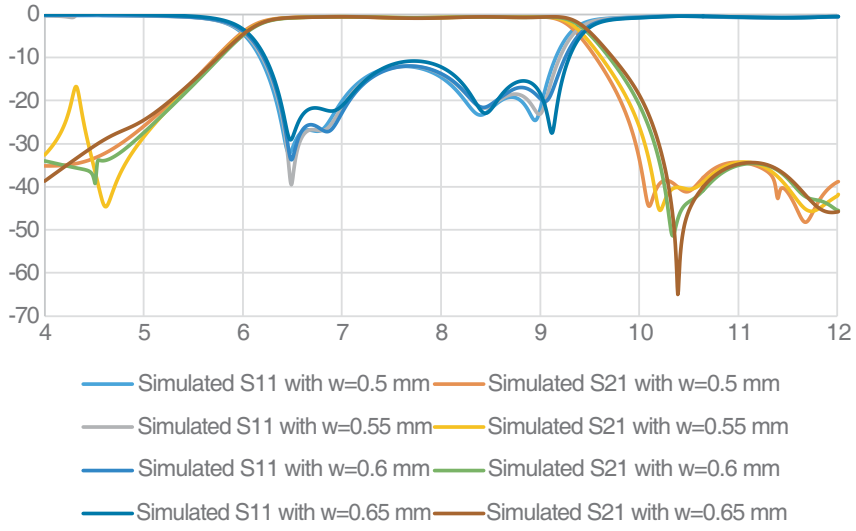

(d)

Figure 5. (a) Proposed band-pass filter. (b) E-field distribution. (c) S-parameter simulation results and (d) effect of width of the corrugated grooves (W) on S-parameter simulation results.

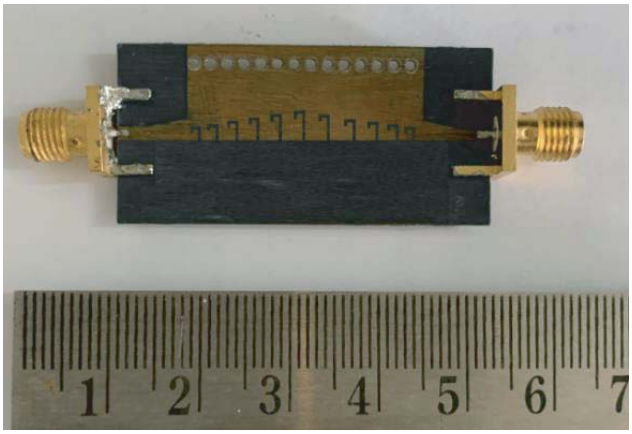

Figure 6. Fabricated structure of proposed filter.

3. OUTCOMES AND DISCUSSION

In the proposed design, an ultra-wideband band-pass filter is designed, simulated, and fabricated on a substrate of Rogers RT/Duroid 5880 with a thickness of 0.508 mm, relative permittivity of 2.2, and loss tangent of 9×10^{-4}. Furthermore, the measurement of the proposed structure is performed on a Keysight N5245A vector network analyser. The proposed filter has the size of $1.67\lambda g \times 0.85\lambda g$ excluding the feeding line, where λg is the guided wavelength at a center frequency of 7.95 GHz. Firstly, the HMSIW structure is designed and simulated, and simulation results show the high-pass response in the desired frequency band. In order to obtain the band-pass response, the HMSIW with high-pass response is combined with the SSPPs with stop-band response. Figure 6 shows a picture of the fabricated structure of the proposed design. In Figure 7, simulated and measured S-parameter results of the designed filter are presented. Moreover, a performance comparison between the designed filter and previously issued work is tabulated in Table 3.

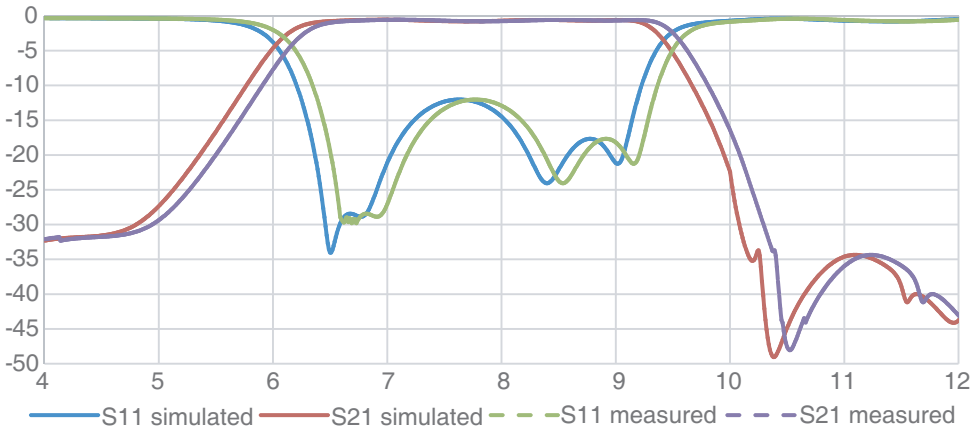

Figure 7. Simulated and measured S-parameter results of the proposed filter.

Table 3. Performance comparison between the presented work and the previously published work.

Reference	Center Frequency (GHz)	Fractional Bandwidth (FBW) %	Insertion loss (dB)	Return loss (dB)	Size
[18]	16.73	57.50	< 1.5	> 10	$11.11\lambda g \times 1.78\lambda g$
[19]	9.25	44	2	> 12	$4.57\lambda g \times 0.91\lambda g$
[20]	3.6	NG	< 2	> 10	$6.17\lambda g \times 0.95\lambda g$
[21]	15.25	49	> 1.1	> 10	NG
[22]	11.1	55	1.2	> 11	$1.03\lambda g \times 0.55\lambda g$
This work	7.85	**44.02**	< 1.25	> 10	$\mathbf{1.67\lambda g \times 0.85\lambda g}$

4. CONCLUSIONS

An ultra-wideband band-pass filter using HMSIW technique is proposed in this paper. Initially, q basic HMSIW structure is designed and simulated. In order to obtain the wide-band band-pass response, SSPPs are introduced in the HMSIW structure. Furthermore, the proposed design is fabricated and tested for functional performance verification. The measured results match well with the simulated ones. The measured result exhibits return loss better than -10 dB and insertion loss less than 1.25 dB with 3 dB fractional bandwidth (FBW) of 44.02% at the center frequency of

7.95 GHz. Furthermore, individual tuning of the lower and upper cut-off frequencies by varying the filter dimensions is demonstrated. Finally, the designed filter exhibits advantages like wide-band response (FBW = 44.02%), compact size (half the typical SIW), low insertion loss, and high return loss. Moreover, tuning over a wide band (FBW = 44.02% to 71.65%) is possible with a slight variation in the physical structure. The proposed filter is well suited for our RADAR application, and it can also be utilized for the other applications in the field of microwave and millimeter-wave.

REFERENCES

1. Brown, B. K., et al., "Traffic radar system," U.S. Patent No. 4,335,382, Jun. 15, 1982.
2. Held, G., *Inter-and Intra-vehicle Communications*, CRC Press, 2007.
3. Marcuvitz, N., *Waveguide Handbook*, No. 21. IET, 1951.
4. Pozar, D. M., *Microwave Engineering*, John Wiley & Sons, 2011.
5. Xu, F. and K. Wu, "Guided-wave and leakage characteristics of substrate integrated waveguide," *IEEE Transactions on Microwave Theory and Techniques*, Vol. 53, No. 1, 66–73, 2005.
6. Bozzi, M., A. Georgiadis, and K. Wu, "Review of substrate-integrated waveguide circuits and antennas," *IET Microwaves, Antennas & Propagation*, Vol. 5, No. 8, 909–920, 2011.
7. Ritchie, R. H., "Plasma losses by fast electrons in thin films," *Physical Review*, Vol. 106, No. 5, 874, 1957.
8. Barnes, W. L., A. Dereux, and T. W. Ebbesen, "Surface plasmon subwavelength optics," *Nature*, Vol. 424, No. 6950, 824–830, 2003.
9. Maier, S. A., *Plasmonics: Fundamentals and Applications*, Springer Science & Business Media, 2007.
10. Shen, X. and T. J. Cui, "Planar plasmonicmetamaterial on a thin film with nearly zero thickness," *Applied Physics Letters*, Vol. 102, No. 21, 211909, 2013.
11. Mahant, K. and H. Mewada, "A novel Substrate Integrated Waveguide (SIW) based highly selective filter for radar applications," *Journal of Electromagnetic Waves and Applications*, Vol. 33, No. 13, 1718–1725, 2019.
12. Mahant, K. and H. Mewada, "Substrate integrated waveguide based bandpass filter with defected ground structure for FMCW radar application," *International Journal of Sensors Wireless Communications and Control*, Vol. 10, No. 3, 421–429, 2020.
13. Khorand, T. and M. Sajjad Bayati, "Novel half-mode substrate integrated waveguide bandpass filters using semi-hexagonal resonators," *AEU — International Journal of Electronics and Communications*, Vol. 95, 52–58, 2018.
14. Mahant, K., et al., "HMSIW based highly selective filter for radar applications," *Circuit World*, 2020.
15. Máximo-Gutiérrez, C., J. Hinojosa, and A. Alvarez-Melcon, "Design of wide band-pass Substrate Integrated Waveguide (SIW) filters based on stepped impedances," *AEU — International Journal of Electronics and Communications*, Vol. 100, 1–8, 2019.
16. Mahant, K. and H. Mewada, "Substrate Integrated Waveguide based dual-band bandpass filter using split ring resonator and defected ground structure for SFCW Radar applications," *International Journal of RF and Microwave Computer-Aided Engineering*, Vol. 28, No. 9, e21508, 2018.
17. Patel, A., et al., "Design of highly selective bandpass filters for communication between two satellites at K band frequency," *2015 IEEE 16th Annual Wireless and Microwave Technology Conference (WAMICON)*, IEEE, 2015.
18. Zhang, Q., et al., "A hybrid circuit for spoof surface plasmons and spatial waveguide modes to reach controllable band-pass filters," *Scientific Reports*, Vol. 5, No. 1, 1–9, 2015.
19. Chen, P., et al., "Hybrid spoof surface plasmonpolariton and substrate integrated waveguide broadband bandpass filter with wide out-of-band rejection," *IEEE Microwave and Wireless Components Letters*, Vol. 28, No. 11, 984–986, 2018.

20. Mittal, G. and N. P. Pathak, "Spoof surface plasmonpolaritons based microwave bandpass filter," *Microwave and Optical Technology Letters*, Vol. 63, No. 1, 51–57, 2021.
21. Rudramuni, K., et al., "Compact bandpass filter based on hybrid spoof surface plasmon and substrate integrated waveguide transmission line," *2017 IEEE Electrical Design of Advanced Packaging and Systems Symposium (EDAPS)*, IEEE, 2017.
22. Singh, N., et al., "Substrate integrated waveguide wideband and ultra-wideband bandpass filters using multimode resonator," *Advances in VLSI, Communication, and Signal Processing*, 579–586, Springer, Singapore, 2020.